Magnetic susceptibility contributions and electronic density of states in $(Ti,Zr)_{100-x}(Ni,Cu)_x$ metallic glasses and crystalline compounds

S. Mankovsky,[1,*] I. Bakonyi,[2] and H. Ebert[1]
[1]*Department Chemie und Biochemie/Physikalische Chemie, Universität München, Butenandtstrasse 5-13, D-81377 München, Germany*
[2]*Research Institute for Solid Sate Physics and Optics, Hungarian Academy of Sciences, P.O. Box 49, H-1525 Budapest, Hungary*
(Received 20 September 2006; revised manuscript received 25 May 2007; published 6 November 2007)

Available experimental data on the magnetic susceptibility of melt-quenched amorphous TE-TL alloys (TE=Ti or Zr; TL=Ni or Cu) and the corresponding crystalline counterparts are reviewed. In order to analyze the composition dependence of the magnetic susceptibility in these systems, the individual contributions (element-resolved Langevin diamagnetic, Van Vleck and Pauli spin susceptibility, as well as the Landau susceptibility) were determined directly by theoretical calculations for these TE-TL alloys in a face-centered-cubic (fcc) structure. The total susceptibility, both experimental and calculated, was found to decrease with increasing TL content up to about 60–70 at. %. This variation was mainly ascribed to corresponding changes of the Van Vleck contribution and the spin susceptibility. The composition dependence of the latter term is in line with the previously established trend of variation of the density of states at the Fermi level $n(E_F)$ upon alloying. As in previous reports on electronic band-structure calculations, it turned out that to get agreement with experiments on $n(E_F)$ in amorphous Zr-Ni alloys, at least some partial chemical ordering should be taken into account. Available experimental data of crystalline stoichiometric Zr-Ni compounds beyond 70 at. % Ni show a gradual increase of the Pauli susceptibility, indicating an approach toward the onset of ferromagnetic order observed previously experimentally around 90 at. % Ni in amorphous Zr-Ni alloys. The susceptibility calculations for fcc Ti-Ni and Zr-Ni alloys indicate a strong increase of the spin susceptibility component above 70 at. % Ni, and the calculated Stoner enhancement for $Zr_{10}Ni_{90}$ fulfills the condition of ferromagnetism in agreement with the experimental observation.

DOI: 10.1103/PhysRevB.76.184405 PACS number(s): 75.30.Cr, 71.55.Jv, 75.40.Cx, 71.20.Be

I. INTRODUCTION

Alloys of early transition metals (TE) with late transition metals (TL) such as, e.g., Zr-Ni or Ti-Cu can be prepared in an amorphous state for a wide concentration range by melt quenching and the physical properties of TE-TL metallic glasses have been studied extensively. In a previous work,[1] we have summarized experimental data on the low-temperature specific heat and superconductive properties of paramagnetic $TE_{100-x}TL_x$ $(20 \leqslant x \leqslant 70)$ amorphous alloys with TE=Ti and Zr and TL=Ni and Cu. The electronic density of states (DOS) $n(E_F)$ at the Fermi level deduced from the experimental data was found to decrease monotonically with TL content x in this concentration range. The results of theoretical band-structure calculations reported for the same amorphous alloys in the literature[2] were in good agreement with the experimental values, concerning both the magnitude of $n(E_F)$ and its composition dependence.

This composition dependence of $n(E_F)$ can be explained in terms of the variation of the overall electronic DOS upon alloying in these systems. It has been revealed by photoemission experiments and confirmed by theoretical band-structure calculations[2] that the Ni $3d$ and Cu $3d$ band peaks are positioned well below the Fermi level, while the Ti $3d$ and Zr $4d$ bands are mostly centered at around or even slightly above the Fermi level in these alloys. Consequently, in TE-TL alloy systems, the electronic DOS at E_F is usually dominated by the TE d bands, and with increasing TL=Ni or Cu content (up to about 70 at. % TL), the TE contribution to $n(E_F)$ decreases because the relative positions of the TE and TL bands remain mainly unchanged.

In the present paper, we analyze the composition dependence of the magnetic susceptibility based on experimental data reported in the literature for (Ti,Zr)-(Ni,Cu) amorphous alloys and their crystalline counterparts. For this purpose, theoretical calculations of the individual susceptibility contributions (Langevin diamagnetic, Van Vleck, Landau, and spin susceptibility) were performed for these binary TE-TL alloys in a face-centered-cubic (fcc) structure. In general, the orbital susceptibility contributions are not expected to depend strongly on the local atomic structure. Furthermore, the fcc structure can be considered as a good first approximation of the local topology of the amorphous state in these systems.[1] This way, we could establish that the experimentally observed linear decrease of the magnetic susceptibility in these amorphous alloys up to about 60–70 at. % TL content arises primarily for two reasons. First, the TE elements have a larger Van Vleck contribution and, second, the electronic density of states at the Fermi level $n(E_F)$ is also dominated by these elements in most cases. At the same time, both the Van Vleck and the spin susceptibility contributions to the total susceptibility of the alloys evidently decrease with increasing TL content, i.e., with decreasing TE content. The composition dependence of the latter term (Pauli susceptibility) is in line with the previously established trend[1] of $n(E_F)$ variation upon alloying in the TE-TL systems studied here. Furthermore, available experimental magnetic susceptibility data of crystalline stoichiometric Zr-Ni (and also Hf-Ni) compounds beyond 70 at. % Ni indicate a gradual increase of the Stoner enhancement of the Pauli susceptibility. This enhancement results finally in the onset of ferromagnetic order around 90 at. % Ni as was established recently experimentally.[3,4]

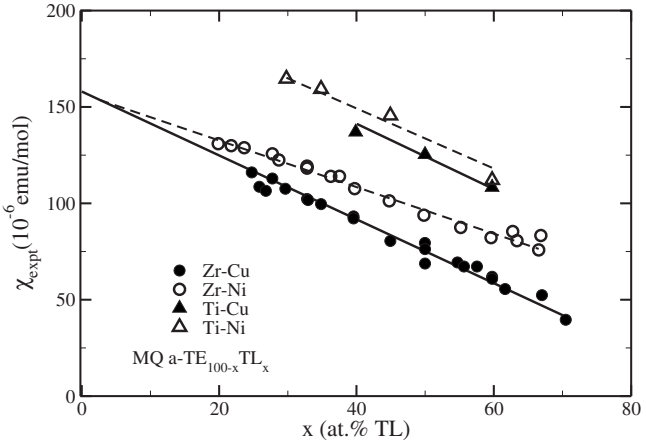

FIG. 1. Composition dependence of the experimental room-temperature magnetic susceptibility χ_{expt} for amorphous Ti-Ni, Ti-Cu, Zr-Ni, and Zr-Cu alloys (for data sources, see text). The straight lines represent linear fits to the data as described in the text with fit parameters given in Eqs. (1) and (2).

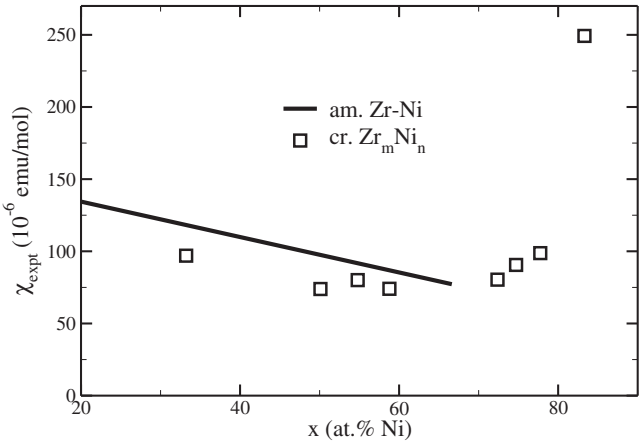

FIG. 2. Composition dependence of the experimental room-temperature magnetic susceptibility χ_{expt} for crystalline stoichiometric Zr_nNi_m intermetallic compounds (□, Ref. 21). The average experimental magnetic susceptibility for amorphous Zr-Ni alloys from Fig. 1 is also indicated by the solid line.

The paper is organized as follows. In Sec. II, the experimental magnetic susceptibility data are summarized, and in Sec. III, the magnetic susceptibility calculation method is presented. In Secs. IV and V, the orbital and spin susceptibility contributions are discussed, respectively. In Sec. VI, the total calculated susceptibility is compared to the experimental data. Section VII finally summarizes the main conclusions of the present work.

II. EXPERIMENTAL MAGNETIC SUSCEPTIBILITY DATA FOR AMORPHOUS (Ti,Zr)-(Ni,Cu) ALLOYS AND CRYSTALLINE Zr-Ni COMPOUNDS

Figure 1 summarizes experimental magnetic susceptibility χ_{expt} data on melt-quenched amorphous paramagnetic TE-TL alloy systems [Ti-Ni (Ref. 5), Ti-Cu (Ref. 6), Zr-Ni (Refs. 7–10), and Zr-Cu (Refs. 8 and 11–15)] as a function of the concentration x of the TL component (Ni or Cu). We have not included the data of Ref. 16 for a-$Zr_{78}Ni_{22}$, a-$Zr_{64}Ni_{36}$, and a-$Zr_{37}Ni_{63}$ (227×10^{-6}, 159×10^{-6}, and 141×10^{-6} emu/mol, respectively) since they are evidently much larger than the rest of the reported data. Such large susceptibility values are usually due to some amount of Ni precipitates in the amorphous matrix. To a lesser extent, the same applies for the χ_{expt} data for a-$Zr_{67}Ni_{33}$ in Ref. 11 ($\chi_{expt}=128\times10^{-6}$ emu/mol) and in Ref. 17 ($\chi_{expt}=127\times10^{-6}$ emu/mol) as well as for a-$Zr_{47.5}Ni_{52.5}$ in Ref. 18 ($\chi_{expt}=100\times10^{-6}$ and 108×10^{-6} emu/mol); therefore, these data will also not be taken into account when discussing the composition dependence of χ_{expt} for the Zr-Ni system. For the Zr-Cu system, only the data for a-$Zr_{43}Cu_{57}$ in Ref. 19 ($\chi_{expt}=83\times10^{-6}$ emu/mol) and for a-$Zr_{40}Cu_{60}$ in Ref. 20 ($\chi_{expt}=40\times10^{-6}$ emu/mol) deviate markedly from the main trend of the experimental results and, therefore, they will be omitted from the discussion.

According to Fig. 1, χ_{expt} decreases approximately linearly with the increase of the TL content for all four alloy systems considered here.

In analyzing the χ_{expt} data, we shall proceed in a way similar as was done for the discussion of the low-temperature specific heat results for the same systems.[1] Namely, when attempting to fit the χ_{expt} data for the Zr-Ni and Zr-Cu systems by a straight line, a common value is assumed for the magnetic susceptibility of hypothetical amorphous Zr (a-Zr) for both systems. The solid and dashed line fits to the data in Fig. 1 were determined under this constraint. The experimental results were then described by the equations

$$\chi_{expt} = 158 - 1.66x \quad \text{(Zr-Cu)}, \tag{1a}$$

$$\chi_{expt} = 158 - 1.23x \quad \text{(Zr-Ni)}, \tag{1b}$$

where the susceptibility is in units of 10^{-6} emu/mol, and x gives the TL content in at. %. We can see that a common value of $\chi_{expt}(a\text{-Zr})=155\times10^{-6}$ emu/mol for both the Zr-Cu and Zr-Ni alloys provides a good fit of the available experimental susceptibility data. Fitting separately the Zr-Cu and Zr-Ni data gave very similar fit parameters and the fit quality increased only slightly.

Although the number of available magnetic susceptibility data is much less for the Ti-Cu and Ti-Ni alloy systems, we could apply the same type of fit to these data as for the Zr-based alloys. Constraining a common value of $\chi_{expt}(a\text{-Ti})=211\times10^{-6}$ emu/mol for both the Ti-Cu and Ti-Ni alloys leads to the following fit parameters for the available experimental susceptibility data:

$$\chi_{expt} = 211 - 1.73x \quad \text{(Ti-Cu)}, \tag{2a}$$

$$\chi_{expt} = 211 - 1.54x \quad \text{(Ti-Ni)}. \tag{2b}$$

Amamou *et al.*[21] reported magnetic susceptibility data for a large number of stoichiometric crystalline Zr_mNi_n compounds. These are shown in Fig. 2 where, for comparison, the fitted data for amorphous Zr-Ni alloys (solid line) according to Eq. (1b) are also included. The susceptibility data for crystalline stoichiometric Zr-Ni compounds with Ni contents

below 70 at. % are somewhat smaller than the values of the corresponding amorphous alloys. The same behavior was observed for the available electronic specific heat data.[1] On the other hand, the magnetic susceptibility data in Fig. 2 for the crystalline Zr-Ni compounds above 70 at. % Ni show a steep rise, again in agreement with electronic specific heat behavior.[1] The magnetic susceptibility of both amorphous[7–9] and crystalline[21] Zr-Ni alloys exhibits weak or negligible temperature dependence up to 78 at. % Ni (crystalline phase Zr_2Ni_7). For the intermetallic compound $ZrNi_5$ (83.3 at. % Ni), the magnetic susceptibility is much larger with its room-temperature value of $\chi_{\text{expt}}(300\ \text{K})=247\times10^{-6}$ emu/mol.[21] For a nanocrystalline $Hf_{11}Ni_{89}$ alloy with the $HfNi_5$ structure, corresponding to a higher Ni content, an even larger susceptibility, $\chi_{\text{expt}}(300\ \text{K})=360\times10^{-6}$ emu/mol, was reported.[4] Both latter alloys remained, however, Pauli paramagnetic down to at least 5 K.[4,21,22] Nevertheless, the magnitude of the magnetic susceptibility of both alloys and the observed temperature dependence of the susceptibility of the $ZrNi_5$ compound[21] strongly resemble the behavior of exchange (Stoner) enhanced Pauli paramagnets such as Pd metal,[23] the latter having a room-temperature susceptibility of $\chi_{\text{expt}}(300\ \text{K})=552\times10^{-6}$ emu/mol.

The susceptibility data beyond 70 at. % Ni in the Zr-Ni (and Hf-Ni) system indicate the onset of spin fluctuations and an approach to ferromagnetism. Indeed, Zr-Ni alloys were found to exhibit spontaneous magnetic order above about 89.5 at. % Ni (Refs. 3 and 4) in the form of very weak itinerant ferromagnetism.

III. CALCULATION OF THE MAGNETIC SUSCEPTIBILITIES

A. Theoretical framework for the calculation of the magnetic susceptibility

To calculate the magnetic susceptibility, a combination of linear response theory and the fully relativistic version of the Green's function technique was used following the work of Staunton[24] and Ebert and co-workers.[25] The magnetic susceptibility includes spin and orbital parts which are coupled due to the spin-orbit interaction[25–27] and, therefore, they have to be determined simultaneously. Within the approach described in Refs. 24 and 25, the electronic Green's function $G^B(\mathbf{r},\mathbf{r}',E)$ of a paramagnetic solid in the presence of an external magnetic field B_{ext} can be represented in terms of the field-free Green's function $G(\mathbf{r},\mathbf{r}',E)$ and a perturbation $\Delta\mathcal{H}$ by the Dyson equation

$$G^B = G + G\Delta\mathcal{H}G^B. \tag{3}$$

In a linear approximation of perturbation theory, G^B takes the form

$$G^B = G + G\Delta\mathcal{H}G. \tag{4}$$

In the present work, the field-free Green's function $G(\mathbf{r},\mathbf{r}',E)$ describing the electronic structure of an alloy ground state was calculated within the relativistic Korringa-Kohn-Rostoker band-structure method in connection with the coherent potential approximation alloy theory. This scheme supplies individual information about the electronic structure of all components of an alloy. The local density of states (DOS) of valence electrons for an alloy component, for instance, is determined through the integral over the Wigner-Seitz cell Ω_α of a Green's function $G(\mathbf{r},\mathbf{r}',E)$:

$$n_\alpha(E) = -\frac{1}{\pi}\,\text{Im}\int_{\Omega_\alpha} G(\mathbf{r},\mathbf{r},E)d^3r. \tag{5}$$

Also, the knowledge of the field-free Green's function allows one to express the change of the expectation value $\langle\mathcal{A}\rangle$ of any operator induced by an external magnetic field B_{ext} by the following expression:

$$\Delta\langle\mathcal{A}\rangle_\alpha = -\frac{1}{\pi}\text{Tr}\,\text{Im}\int^{E_F} dE\int_{\Omega_\alpha} d^3r\sum_\beta\int_{\Omega_\beta} d^3r'\,\mathcal{A}G\Delta\mathcal{H}G. \tag{6}$$

In our case, we deal with the induced spin and orbital magnetic moments which, when divided by the value of the external magnetic field B_{ext}, will give us the spin and orbital magnetic susceptibilities. The perturbation $\Delta\mathcal{H}$ in Eqs. (3) and (4) represents the coupling of the spin and orbital motion to the external magnetic field:

$$\Delta\mathcal{H} = \Delta\mathcal{H}_{\text{spin}} + \Delta\mathcal{H}_{\text{orb}}. \tag{7}$$

The spin perturbation $\Delta\mathcal{H}_{\text{spin}}$ includes the Zeeman term as well as a term $\Delta\mathcal{H}^{\text{xc}}_{\text{spin}}$ representing the modified electron-electron interaction due to the induced magnetization:

$$\Delta\mathcal{H}_{\text{spin}}(\mathbf{r}) = \beta\sigma_z\mu_B B_{\text{ext}} + \Delta\mathcal{H}^{\text{xc}}_{\text{spin}}(\mathbf{r}). \tag{8}$$

Here, β is one of the standard Dirac matrices and σz is the z component of the Pauli spin operator.[25] The first term in Eq. (8) gives rise, according to Eq. (6), to the so-called unenhanced Pauli spin susceptibility. The second term, the so-called feedback term, is given within spin-density functional theory by the change in the spin-dependent exchange-correlation potential due to the spin magnetization:[28,29]

$$\Delta\mathcal{H}^{\text{xc}}_{\text{spin}}(\mathbf{r}) = \beta\sigma_z K^{\text{xc}\alpha}_{\text{spin}}(\mathbf{r})\gamma^\alpha(\mathbf{r})\chi^\alpha_{\text{spin}}\mu_B B_{\text{ext}}. \tag{9}$$

It was assumed in this equation that under a small perturbation, $\Delta\mathcal{H}^{\text{xc}}_{\text{spin}}(\mathbf{r})$ depends linearly on the induced spin magnetization $m^\alpha_{\text{spin}}(\mathbf{r})=\gamma^\alpha(\mathbf{r})\chi^\alpha_{\text{spin}}B_{\text{ext}}$, with $\gamma_\alpha(\mathbf{r})$ denoting the normalized spin density, $\chi^\alpha_{\text{spin}}$ is the local spin susceptibility for site α, and $K^{\text{xc}\,\alpha}_{\text{spin}}(\mathbf{r})$ is the corresponding interaction kernel.[28] To make use of the expression given in Eq. (9), first of all, one has to determine the unknown local susceptibility $\chi^\alpha_{\text{spin}}$.

For a one-component system, within a nonrelativistic treatment (when the Pauli spin susceptibility only contributes to the spin susceptibility χ_{spin}), the spin susceptibility is given by the well-known expression

$$\chi_{\text{spin}} = S\chi^0_{\text{spin}} = \frac{1}{1-In(E_F)}\chi^0_{\text{spin}}, \tag{10}$$

where $\chi^0_{\text{spin}}=\mu_B^2 n(E_F)$ is the unenhanced Pauli spin susceptibility, I denotes the Stoner exchange-correlation integral, and S is the Stoner enhancement factor.

In the case of a one-component system, the Stoner exchange-correlation integral is determined by the local charge density and induced spin magnetic moment [through $K^{\mathrm{xc}}_{\mathrm{spin}}(\mathbf{r})$ and $\gamma(\mathbf{r})$ in Eq. (9)]. However, in the case of an alloy system, the induced spin magnetic moments $m^{\alpha}_{\mathrm{spin}}(\mathbf{r})$ of the alloy components α have to be considered separately. The value of the induced spin magnetic moment of a component β in this case is determined not only by its local unenhanced magnetic susceptibility and local Stoner enhancement factor (as in the case of one-component system). According to Eqs. (6) and (8), the induced spin magnetic moment of the alloy component α creates an additional contribution to the magnetic moment of the component β [see the Appendix, Eqs. (A1) and (A2)]. This coupling of the induced spin magnetic moments m_{α} and m_{β} on different sites gives rise to an intercomponent cross term for the magnetic susceptibility $\chi^{0}_{\alpha\beta}$ [Eq. (A4)], leading to a corresponding coupling of the partial magnetic susceptibilities of the different alloy components [Eq. (A3)]. For that reason, the element-projected magnetic susceptibility in an alloy has to be determined from the solution of a system of equations for the coupled magnetic susceptibilities of all alloy components. As a result, the effective enhancement factor for the spin susceptibility of each alloy component, obtained from the solution of system of equations, is determined not only by the Stoner exchange-correlation factors of the corresponding alloy component but also by the enhancement through the intercomponent interaction (see the Appendix). Below, we will discuss this effect for the (Ti, Zr)-(Cu.Ni) alloys.

The total orbital susceptibility χ^{tot}_{o} includes three components: diamagnetic Langevin susceptibility χ_{dia}, Landau susceptibility χ_{L}, and paramagnetic Van Vleck susceptibility χ_{orb}:

$$\chi^{\mathrm{tot}}_{o} = \chi_{\mathrm{dia}} + \chi_{L} + \chi_{\mathrm{orb}}. \tag{11}$$

First, let us discuss the Van Vleck susceptibility. It is caused by a perturbation $\Delta\mathcal{H}_{\mathrm{orb}}$ that can be split, in analogy to Eq. (8), into two terms:

$$\Delta\mathcal{H}_{\mathrm{orb}} = \beta I_{z}\mu_{B}B_{\mathrm{ext}} + \Delta\mathcal{H}^{\mathrm{xc}}_{\mathrm{orb}}. \tag{12}$$

Here, l_z is the z component of the orbital angular momentum operator and $\Delta\mathcal{H}^{\mathrm{xc}}_{\mathrm{orb}}$ is approximated here by the so-called Brooks' orbital polarization term[31] describing the Stoner-like enhancement of the orbital susceptibility. It depends linearly on the local orbital susceptibility $\chi^{\alpha}_{\mathrm{orb}}$.

Within a nonrelativistic formalism, the spin and orbital degrees of freedom in paramagnetic systems are completely decoupled. However, as was pointed out by Yasui and Shimizu,[27] the presence of a spin-orbit coupling leads to a coupling of induced spin and orbital magnetic moments and creates the additional terms of magnetic susceptibility, χ_{so} and χ_{os}.[25,27] Due to these terms, a coupling of an external field to the orbital (spin) degree of the electrons gives rise to an induced spin (orbital) magnetization. Thus, in the general case, the local susceptibilities χ^{α}_{s} and χ^{α}_{o} of complex systems have to be found from the solution of a system of linear equations derived from the perturbative expressions of the induced spin and orbital magnetic moments. The spin and orbital susceptibilities are represented in this case by two terms:

$$\chi_{s} = \chi_{\mathrm{spin}} + \chi_{\mathrm{so}},$$

$$\tilde{\chi}_{\mathrm{orb}} = \chi_{\mathrm{orb}} + \chi_{\mathrm{os}}. \tag{13}$$

Here, the total spin susceptibility is denoted by χ_s, whereas the term χ_{spin} corresponds to the spin susceptibility in Eq. (10) which arises from the (Stoner-enhanced) Pauli susceptibility χ_P and it is due to the spin source term $\Delta\mathcal{H}_{\mathrm{spin}}$. The orbital susceptibility denoted by χ_{orb} (also called Van Vleck susceptibility χ_{VV}) arises due to the orbital source term $\Delta\mathcal{H}_{\mathrm{orb}}$. In the following discussion in the next paragraphs, we will use the notation χ_{VV} for the orbital susceptibility term $\tilde{\chi}_{\mathrm{orb}}$ to stress its leading role among the orbital susceptibility contributions and to distinguish it from the orbital Langevin and Landau susceptibilities. The cross terms χ_{so} and χ_{os}, on the other hand, stem from the terms $\Delta\mathcal{H}_{\mathrm{orb}}$ and $\Delta\mathcal{H}_{\mathrm{spin}}$, respectively.

To study the magnetic susceptibility of disordered alloys, one has to deal with the configurational averages for expressions of the type $\langle AGBG\rangle$, with A and B being arbitrary operators. The problem of calculating these averages has been discussed by Staunton[24] (when A, $B=\beta\sigma_z$) and Butler[30] (when A, $B=\mathbf{j}$, i.e., the current density operator). For the application below, it turned out that the approximation $\langle AGBG\rangle \cong \langle AG\rangle\langle BG\rangle$ is well justified.

As was already mentioned above [see Eq. (11)], the Van Vleck orbital susceptibility χ_{VV} has to be complemented by the corresponding diamagnetic Langevin susceptibility and Landau susceptibility, χ_L and χ_{dia}, respectively. These latter two terms have been evaluated by a relativistic formulation of the expressions given by Benkowitsch and Winter.[26] From the work of these authors, it turned out that whereas one always has $\chi_{\mathrm{VV}}>0$ and $\chi_{\mathrm{dia}}<0$, for transition metals, χ_L may be either positive or negative and may be of the same order of magnitude as χ_{dia} (the Landau result $\chi_L=-\chi_P/3$ is valid for a free-electron gas only[32]). Furthermore, it was found[26] that since all occupied electronic states within the Wigner-Seitz cell must be included when accounting for χ_{dia}, this term contains contributions not only from core electrons but also from valence electrons:

$$\chi_{\mathrm{dia}} = \chi_{\mathrm{dia,core}} + \chi_{\mathrm{dia,val}}. \tag{14}$$

Finally, the total susceptibility χ_{tot} to be compared with the experimental data can be written as

$$\chi_{\mathrm{tot}} = \chi_{s} + \chi^{\mathrm{tot}}_{o} = \chi_{\mathrm{spin}} + \chi_{\mathrm{so}} + \chi_{\mathrm{VV}} + \chi_{\mathrm{os}} + \chi_{L} + \chi_{\mathrm{dia}}. \tag{15}$$

B. Application to (Ti,Zr)-(Ni,Cu) alloys

The calculation of the magnetic susceptibility contributions for the (Ti,Zr)-(Ni,Cu) alloys was performed by assuming an fcc crystal structure. The lattice parameter was chosen to give the same atomic volume as reported for the corresponding amorphous alloy composition.[33] Both electronic structure[1] and atomic volume[33] data indicate that the fcc lat-

tice is a good first approximation for the local atomic structure in TE-TL type metallic glasses. High-speed structural transformation studies by x-ray diffraction on an amorphous $Zr_{67}Ni_{33}$ alloy[34] also demonstrated that the very first crystallized phase appearing is the fcc-Zr_2Ni structure. The high (usually 12 or more) first neighbor coordination number of these glasses and the highly isotropic character of the fcc arrangement further support the use of an fcc structure for approximating the amorphous state. The same arguments were applied to justify the choice of an fcc structure also in previous band-structure calculations for TE-TL glasses.[35,36] Whereas the orbital susceptibility contributions are not influenced in an appreciable way by the atomic arrangements anyway, the crystal structure does strongly affect the electronic DOS curve and, thus, via $n(E_F)$ also the spin (Pauli) susceptibility. This was demonstrated by band-structure calculations, e.g., for the different structural modifications of Ti, Zr, and Hf metals.[37] On the other hand, due to the similarity of the atomic arrangements of the amorphous and fcc structures, the DOS curves are also very similar for the two cases with the only difference that the DOS curve of the amorphous state will be a "smeared-out" version of the fcc counterpart.[38] This behavior can be observed, indeed, if we compare the calculated DOS curves for fcc-Ni and liquid Ni,[39] for fcc-Zr,[37] liquid Zr,[39] and amorphous Zr,[40] as well as for fcc-Cu and liquid Cu.[41]

It was also assumed for our calculations that there is no chemical short-range order (CSRO) in the alloys investigated, i.e., the chemical environment of the first neighbor shell of each atom reflects the average alloy composition. An analysis of the composition dependence of atomic volumes of metallic glasses revealed[33] that the amorphous Ti-Cu and Zr-Cu alloys exhibit an ideal solid solution behavior, hinting at the lack of chemical ordering. In contrast, the atomic volume data[33] suggested a deviation from the ideal solid solution behavior for the Zr-Ni glassy alloys, indicating the presence of a CSRO. In line with these observations, the absence of CSRO was confirmed by theoretical calculations[42] for amorphous Zr-Cu alloys with 33, 50, and 66 at. % Cu based on a structural model using a Bethe lattice in which every atom is located in an fcc environment. On the other hand, for the same composition range of amorphous Zr-Ni alloys, it was concluded[42] that there is a CSRO with preferential unlike first neighborhood which gradually increases with increasing Ni content. Previous diffraction experiments[43] similarly indicated an increase of the CSRO for amorphous Zr-Ni alloys, and even the quantitative agreement of the calculated and experimental CSRO parameters was fairly good. The development of a CSRO in amorphous TE-Ni alloys was also confirmed by molecular dynamic simulations.[44]

It follows from the above considerations that the assumption of an fcc structure without CSRO will certainly be a good approximation for the present susceptibility calculations for the amorphous Ti-Cu and Zr-Cu alloys, but this approach may not be able to properly account for every aspect of the amorphous Ti-Ni and Zr-Ni alloys, especially around and above 50 at. % due to the neglect of CSRO. For this reason, some attempts will be made at least for the Zr-Ni alloys system to take into account the influence of partial chemical ordering.

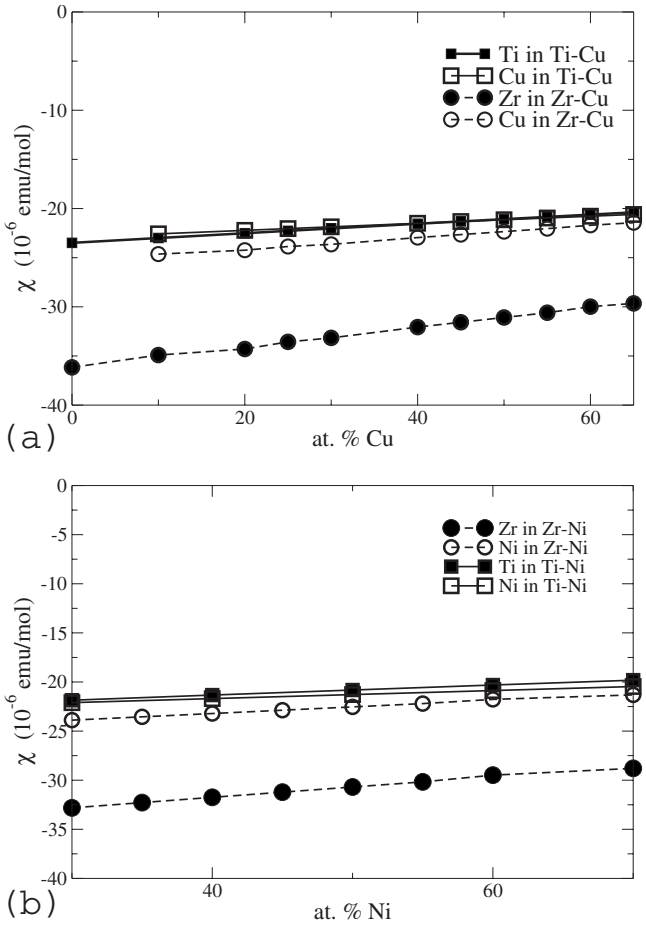

FIG. 3. Calculated diamagnetic susceptibility χ_{dia} for (a) fcc Ti-Cu and fcc Zr-Cu alloys as a function of the Cu content and (b) fcc Ti-Ni and fcc Zr-Ni alloys as a function of the Ni content.

IV. ORBITAL SUSCEPTIBILITY CONTRIBUTIONS

A. Results for the orbital susceptibilities

The diamagnetic susceptibility χ_{dia} was calculated by Banhart *et al.*[45] for pure metals with $Z \leqslant 49$. The values of χ_{dia} derived in the way described above were found to differ from the free-atom and free-ion susceptibilities,[46] in some cases by as much as 20×10^{-6} emu/mol. The calculated χ_{dia} values of Banhart *et al.*[45] are -23×10^{-6} emu/mol for fcc-Ti, -36×10^{-6} emu/mol for bcc-Zr, -19×10^{-6} emu/mol for fcc-Ni, and -19×10^{-6} emu/mol for fcc-Cu. It was shown for the Cu-Rh alloy system[45] that although χ_{dia} varies slightly with composition in a linear manner, its value in a binary alloy may be taken as a composition-weighted average of the pure metal values.

The results of our calculations for χ_{dia} are summarized in Fig. 3. In agreement with previous results,[45] the element-resolved susceptibility contribution χ_{dia} shows a small linear change with composition for all four alloy systems. The contribution of a given type of atoms depends only very weakly on the kind of the other alloy component. The calculated pure Ti, Zr, Ni, and Cu metal values reproduce very well the earlier results of Banhart *et al.*[45]

The calculated Landau susceptibility (χ_L) values are presented in Fig. 4, showing a strong composition dependence

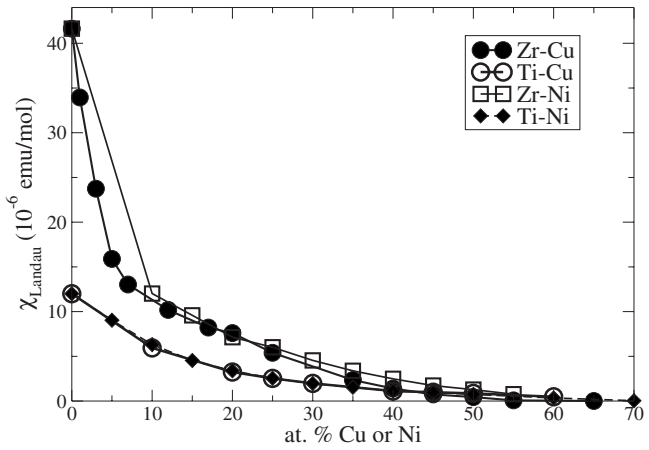

FIG. 4. Calculated Landau susceptibility χ_L for fcc Ti-Cu, Zr-Cu, Ti-Ni, and Zr-Ni alloys as a function of the TL content (TL=Ni or Cu).

on the TE-rich side, especially for TE=Zr, and approaching zero at around the equiatomic composition for all alloy systems. It is also seen that χ_L can indeed be positive and comparable in magnitude to χ_{dia} of the pure TE elements.

The element-resolved calculated Van Vleck susceptibilities χ_{VV} including here also the term χ_{dia} are shown in Fig. 5(a) for the Ti-Cu and Zr-Cu systems. The χ_{VV} contribution of the constituent elements changes only little with Cu content. The χ_{VV} value is much larger for the TE elements due to the partially filled d bands than for Cu having practically completely filled d bands. The value of χ_{VV}(Cu) is approximately the same for the Ti-Cu and Zr-Cu systems, and this indicates a good consistency of our calculated data. Its magnitude is about 20×10^{-6} emu/mol and slightly decreases with increasing Cu content. Concerning the TE contribution to the Van Vleck susceptibility, for the concentrations of interest, we can see that $\chi_{VV}(\text{Ti})\approx90\times10^{-6}$ emu/mol and $\chi_{VV}(\text{Zr})\approx60\times10^{-6}$ emu/mol.

Figure 5(b) shows the Van Vleck susceptibility contributions including also the term χ_{os} for the Ti-Ni and Zr-Ni alloy components. As for the Cu-based alloys above, the TE contributions remain fairly constant with alloy composition at nearly the same values, also here with $\chi_{VV}(\text{Ti})>\chi_{VV}(\text{Zr})$. On the other hand, in both Ni-based alloys, the Ni contribution is comparable to or even larger than the TE contribution and shows a clear decrease with increasing Ni content; furthermore, its value depends to some extent on the alloying partner (Ti or Zr).

The composition dependence of the resulting total Van Vleck susceptibility including also the χ_{so} term is shown in Fig. 5(c) for the four alloy systems. Due to the differences in the composition dependences of the Cu and Ni contributions, the Van Vleck susceptibility shows a decrease for both Cu alloys with increasing Cu content, whereas it exhibits a shallow maximum somewhat below the equiatomic composition as a function of the Ni content. With reference to Fig. 4, we can see from Fig. 5(c) that in comparison with the alloy Van Vleck susceptibility, the Landau term can be neglected for TL compositions above about 50 at. % only.

Finally, we give some figures to illustrate the relative importance of the susceptibility corrections due to the spin-

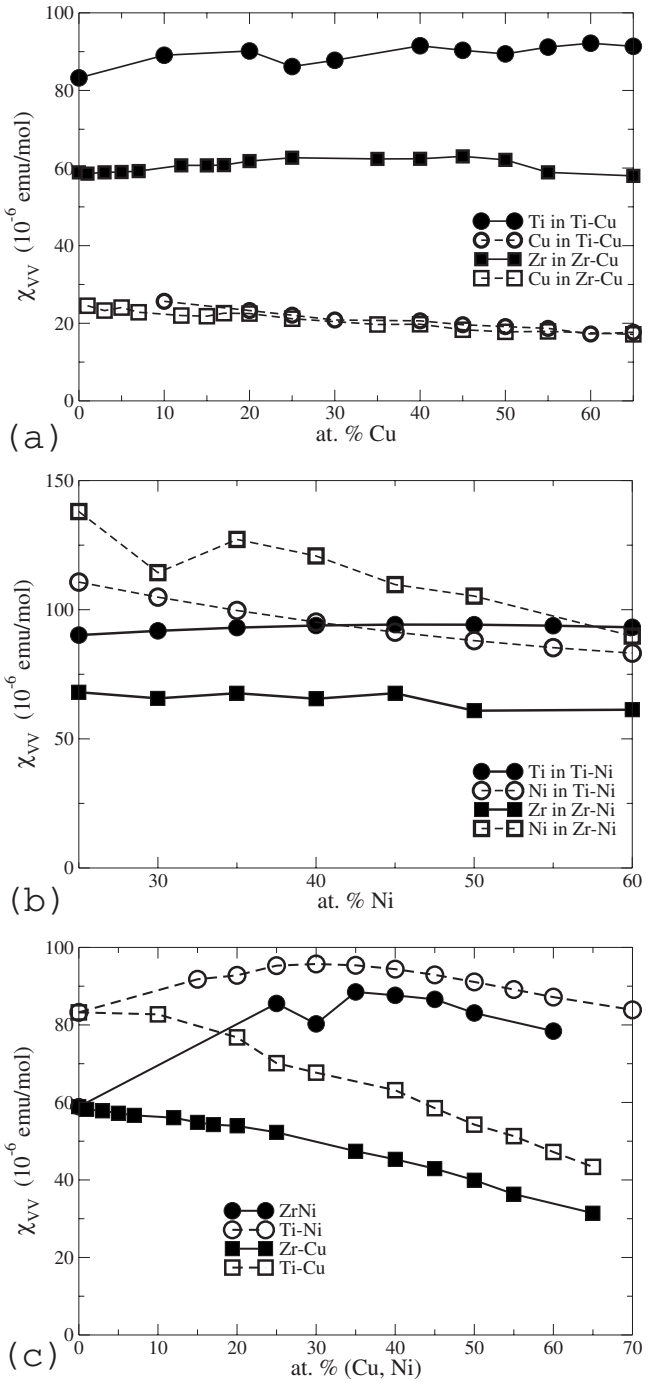

FIG. 5. Calculated Van Vleck susceptibility χ_{VV} for the four alloy systems as a function of the Cu or Ni content: (a) element-resolved χ_{VV} for fcc Ti-Cu and fcc Zr-Cu alloys, (b) element-resolved χ_{VV} for fcc Ti-Ni and fcc Zr-Ni alloys, and (c) comparison of the alloy Van Vleck susceptibility for the four systems. It should be noted that the χ_{VV} values displayed in these graphs include also the spin-orbit coupling term χ_{OS}.

orbit coupling. For the equiatomic Zr-Ni alloy, we calculated $\chi_{\text{so}}=2.7\times10^{-6}$ emu/mol and $\chi_{\text{os}}=6.0\times10^{-6}$ emu/mol. These values should be compared to the corresponding susceptibility values $\chi_s=76\times10^{-6}$ emu/mol and $\chi_{VV}=60\times10^{-6}$ emu/mol, respectively. For the spin susceptibility, the correction is fairly small (abut 4%), whereas it is already

TABLE I. Sum of the Van Vleck and Landau susceptibilities, $\chi_{VV}+\chi_L$, for the different structural modifications of Ti, Zr, and Hf metals. The data for the ω, α, and β phases are estimates from Ref. 37 obtained from previously reported experimental values by correcting for χ_{dia} and χ_{spin} (the two values for the β phase of Ti and Zr refer to two different experimental susceptibility values). The brackets $\langle\ \rangle$ indicate an average of the estimated values over the three different existing crystal structures. The last row gives the values calculated in the present work for the hypothetical fcc phase.

	$\chi_{VV}+\chi_L$ (10^{-6} emu/mol)		
TE metal phase	Ti	Zr	Hf
ω (hex)	99	94	90
α (hcp)	119	102	91
β (bcc)	96	118	82
	66	113	
$\langle\omega,\alpha,\beta\rangle$	$\langle 90\rangle$	$\langle 107\rangle$	$\langle 88\rangle$
fcc	95. 2	100. 5	

more sizable (10%) for the orbital contribution.

B. Corrections for the orbital susceptibilities

In order to extract from the experimental data the susceptibility contribution related to the Fermi-level DOS, the measured total susceptibility should be corrected for the orbital terms. This procedure has been applied for several amorphous TE-TL alloy systems.[8,10,15,47–49] According to Eq. (15), this requires a knowledge of at least χ_{VV}, χ_L, and χ_{dia}.

It was discussed in the previous section that the diamagnetic correction for metallic systems requires the use of χ_{dia} values calculated according to its definition given in Ref. 26 and this is adopted also here by using the values calculated by Banhart *et al.*[45] The Landau susceptibility has usually been neglected; however, according to our calculated results presented above, this seems to be justified for TE-TL alloys in certain concentration ranges only (e.g., for TL contents above about 50 at. % in the alloys studied here). We have also shown that χ_L is positive and can have quite a significant magnitude for pure TE metals (Fig. 4). The major contribution among the orbital terms is definitely the Van Vleck susceptibility that may even dominate the total susceptibility for the TE-TL alloys due to the roughly half-filled *d* shells of the TE metals. We have provided data for the χ_{VV} term resolved for the constituent elements. The following considerations are meant to demonstrate the reliability of our calculated χ_{VV} values for the TE metals in their elemental form and, hence, indirectly also for the alloys investigated.

Since quite often the sum of the Van Vleck and the Landau susceptibilities has been used for correcting experimental data when attempting to extract the Pauli susceptibility, we have made an analysis of the χ_{VV} and χ_L terms for pure Ti and Zr metals, where the χ_L term gives a significant contribution.

As Table I shows, our calculated values of the sum $\chi_{VV}+\chi_L$ compare very well with a previous estimate[37] for the different structural modifications of Ti and Zr metals. This hints again for the reliability of our calculated data. We can also see that $\chi_{VV}+\chi_L$ is roughly the same (within 10%) for the three isoelectronic metals, Ti, Zr, and Hf.

It should be noted that by analyzing magnetic susceptibility and NMR Knight shift data, Eifert *et al.*[15] deduced $\chi_{VV}=(125\pm10)\times10^{-6}$ emu/mol for Zr-Cu metallic glasses with compositions ranging from 28 to 62 at. % Cu. This is about twice the value calculated here but in view of the quite different approach, the difference is understandable.

Following the early work of Place and Rhodes,[50] χ_{VV}(Cu) and χ_{VV}(Ni) have usually been assumed to take the values of 0 and 50×10^{-6} emu/mol, respectively. Our above results indicate that in these TE-TL alloys, the Van Vleck contribution of Cu is not negligible and that of Ni is nearly twice the value commonly used for correction.

It should also be noted in connection with the orbital susceptibility corrections that whereas the χ_{dia} term changes fairly linearly with composition, the χ_L term may be strongly composition dependent. Also, the element-resolved as well as the total χ_{VV} contribution is not always constant, but it may be composition dependent as we have seen here for the case of Ni.

V. SPIN SUSCEPTIBILITY

A. Electronic density of states $n(E_F)$ at the Fermi level

In order to get the spin susceptibility via Eq. (10), we should calculate $n(E_F)$. First, we discuss results for the fcc-Ti and fcc-Zr metals. By taking the constraint that the average atomic volume be equal for the fcc and hcp phases ($V_{fcc}=V_{hcp}$) and using experimental atomic volumes for the hcp phases,[33] the fcc lattice parameters assumed for our calculations were 0.4135 nm (Ti) and 0.4533 nm (Zr). With these lattice constants, we calculated $n(E_F)=1.60$ states/eV atom for fcc-Ti and 1.30 states/eV atom for fcc-Zr. The results of former calculations for fcc-Ti are 1.59 states/eV atom [$a_{fcc}=0.4001$ nm (Ref. 51)], 1.82 states/eV atom [$a_{fcc}=0.4096$ nm (Ref. 52)], 1.84 states/eV atom [$a_{fcc}=0.4006$ nm (Ref. 53)], and 1.76 states/eV atom [$a_{fcc}=0.4135$ nm (Ref. 37)]. The results of former calculations for fcc-Zr are 1.28 states/eV atom [$a_{fcc}=0.4403$ nm (Ref. 51)], 1.55 states/eV atom [$a_{fcc}=0.4675$ nm (Ref. 53)], and 1.55 states/eV atom [$a_{fcc}=0.4533$ nm (Ref. 54)]. Looking at these data sets, we can see that the average $n(E_F)$ values for fcc-Ti and fcc-Zr are about 1.7 and 1.4 states/eV atom, respectively. Although the scatter of calculated $n(E_F)$ values (about ±0.1 states/eV atom) is relatively high when comparing the results of different calculations for a given metal, the difference (0.3 states/eV atom) between the averages for fcc-Ti and fcc-Zr is very well reproduced in those works in which calculations were performed for both metals. We can thus establish that our current results are in accordance with previous work. It should be noted that the lower $n(E_F)$ value for fcc-Zr is due to the broadening of the *d* bands with increasing atomic number.

The results of element-resolved $n(E_F)$ calculations for the fcc Ti-Cu and fcc Zr-Cu alloys are shown in Fig. 6 where the

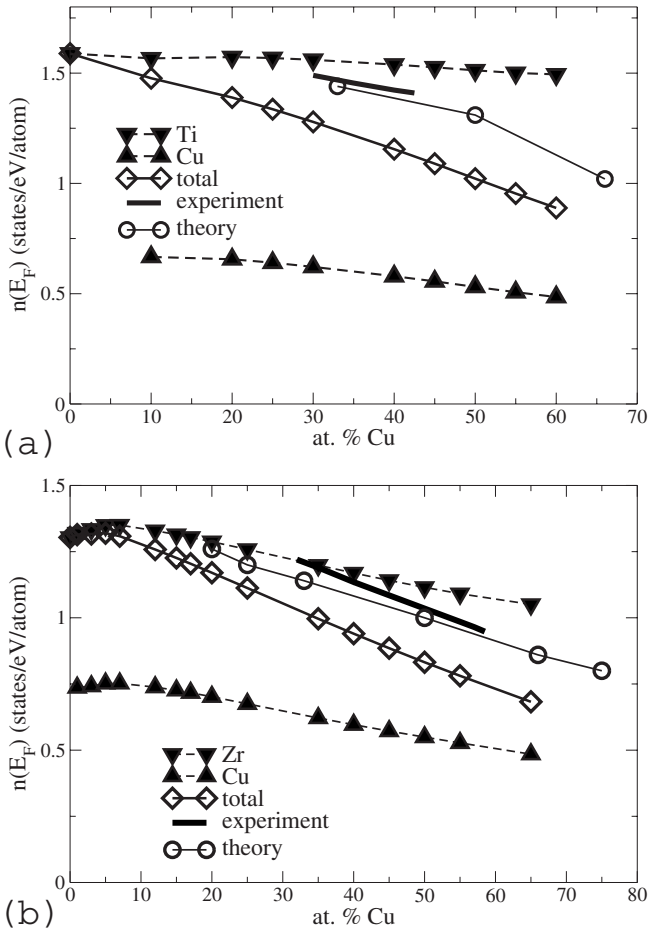

FIG. 6. Element-resolved and total calculated electronic density of states $n(E_F)$ at the Fermi level for fcc (a) Ti-Cu and (b) Zr-Cu alloys as a function of the Cu content. The experimental values (thick solid lines) deduced from electronic specific heat and superconducting data on amorphous Ti-Cu and Zr-Cu alloys (Ref. 1) and some results (symbols ○) of theoretical band-structure calculations on amorphous Ti-Cu (Ref. 55) and Zr-Cu (Refs. 42, 55, and 56) alloys are also included.

composition dependence of the total $n(E_F)$ is also displayed. The thick solid lines indicate the experimental $n(E_F)$ values as deduced from electronic specific heat and superconducting data.[1] Several works[2] have been devoted to electronic band-structure calculations on amorphous Ti-Cu and Zr-Cu alloys, the results of which were summarized in Figs. 9 and 10 of Ref. 1. All these data show a decrease of $n(E_F)$ with increasing Cu content and, apart from one set of results, fall below the experimental data, the difference being for some calculated results as much as 0.3 states/eV atom. From the previous calculated $n(E_F)$ data, we included only those which were reported by Nguyen Manh *et al.*[42,55,56] in Fig. 6 as these are the closest to the experimental data.

As Fig. 7 shows, up to about 60–70 at. % TL content, the behavior of (Ti,Zr)-Ni alloys is very similar to that of the (Ti,Zr)-Cu alloys, i.e., a decrease of $n(E_F)$ with increasing Ni content occurs. In the Ti-Ni system, the only available calculated value from the literature [$a-Ti_{40}Ni_{60}$: $n(E_F)$ = 1.4 states/eV atom (Ref. 58)] and our calculated results for

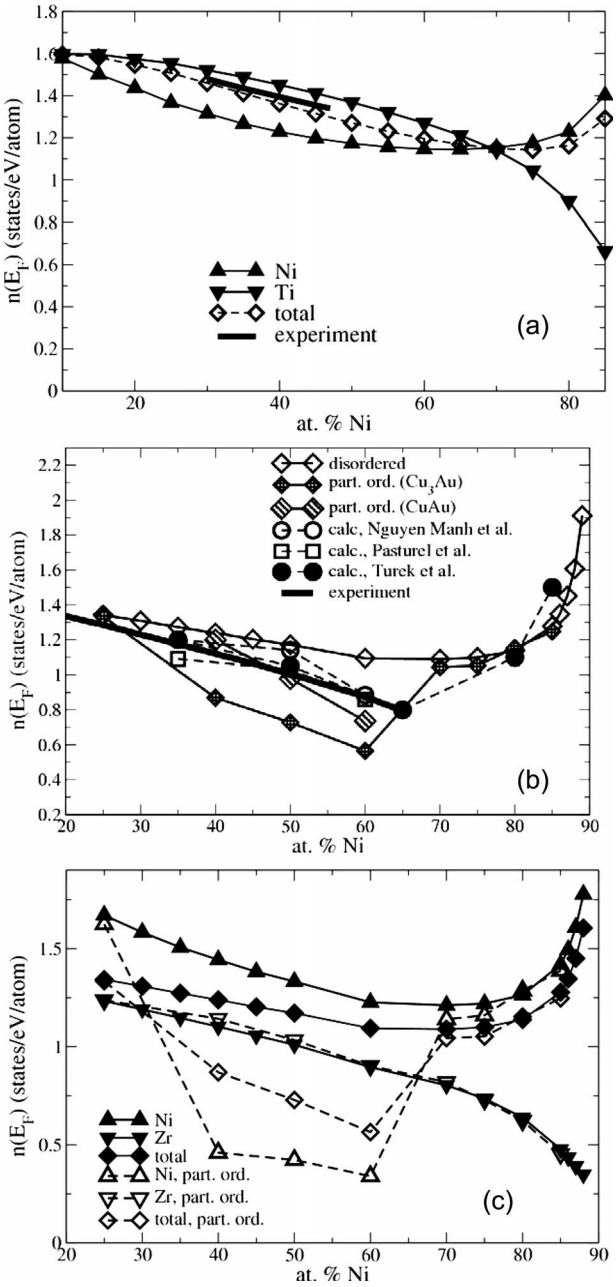

FIG. 7. Calculated element-resolved and total density of states $n(E_F)$ at the Fermi level for fcc (a) Ti-Ni and (b) Zr-Ni alloys as a function of the Ni content. The theoretical results for partially ordered alloys [(b), gray diamonds] as well as the experimental values (thick solid lines) deduced from electronic specific heat and superconducting data on amorphous Ti-Ni and Zr-Ni alloys (Ref. 1) and some results [symbols ○ (Ref. 42), □ (Ref. 57), and ● (Ref. 58)] of theoretical band-structure calculations on amorphous Zr-Ni alloys are also included. (c) The element-projected and total density of states of Zr-Ni alloys in the fully disordered fcc structure (filled symbols) and for the partially ordered state with the Cu_3Au structure (open symbols).

$n(E_F)$ values match very well the experimental data obtained as a lower limit[1] [Fig. 7(a)]. From the results of previous electronic band-structure calculations on amorphous Zr-Ni alloys, which were summarized in Fig. 11 of Ref. 1, we have

selected the data of those studies only[42,57,58] which cover a significant composition range and fall fairly close to the experimental data. In these calculations, the CSRO was properly taken into account. In those studies[42,59] where a comparison was made between results calculated for structures with minimum-energy CSRO and complete chemical disorder, the latter case yielded significantly larger calculated $n(E_F)$ values.

A comparison of our calculated values with the results of former calculations and the experimental data shows that the results of our calculations for (Ti,Zr)-(Ni,Cu) represent well the overall trend of the compositional dependence of $n(E_F)$ in these systems. Nevertheless, there is a slight quantitative difference between our calculated total $n(E_F)$ and the corresponding experimental data in most cases. This difference may be partly attributed to the different atomic arrangements and partly to the neglect of CSRO in our calculations.

In order to show the effects of ordering on the density of states, we also performed calculations for the so-called partially ordered alloys in the Zr-Ni system. Within such calculations, one can simulate different arrangements of alloy components. The calculations have been performed for two different structures: (i) for a CuAu structure (in the concentration region around 50 at. % Ni) with full occupation of one sublattice by the element with dominating concentration, while the second sublattice is occupied by the remaining atoms randomly, and (ii) for a Cu_3Au structure with the Au sublattice always occupied by Ni atoms and the Cu sublattice by the rest of the atoms. The corresponding total DOS at E_F is shown in Fig. 7(b) by differently patterned diamonds. The data we calculated for the partially ordered alloys come very close to the value of the total DOS at the Fermi level of fully disordered alloys when approaching either the Zr-rich or the Ni-rich end of the system. However, the discrepancy between the values of $n(E_F)$ for disordered and partially ordered alloys is fairly large for intermediate concentrations, whereas our values for the partially ordered CuAu state match fairly well the calculated data from the literature [Fig. 7(b)]. As we can see in Fig. 7(c), for the disordered state, $n_{Zr}(E_F) < n_{Ni}(E_F)$ for the whole concentration range, whereas for the partially ordered state (both for the CuAu and the Cu_3Au structures), we have the opposite situation for intermediate concentrations. The latter finding is in agreement with the results of former band calculations[42,57,58] where the CSRO was properly taken into account. Thus, one can conclude that the surroundings of the atoms of alloy components can substantially influence their density of states, especially at Ni concentrations from 40 to 70 at. % Ni. For this reason, a proper consideration of the CSRO is important to achieve a quantitative agreement between the theoretical and experimental values of $n(E_F)$ and χ.

The data for the Ti-Ni and Zr-Ni systems (Fig. 7) indicate that beyond about 60–70 at. % Ni content, the total $n(E_F)$ increases because the Ni d band contribution to the density of states at E_F starts to increase, whereas that of Ti and Zr rapidly decreases here. For compositions around $Zr_{90}Ni_{10}$, no former calculation has been reported and, as Fig. 7(b) indicates, the total $n(E_F)$ value obtained here for the paramagnetic state is already fairly high, leading finally to the appearance of ferromagnetism at this composition as we shall see later.

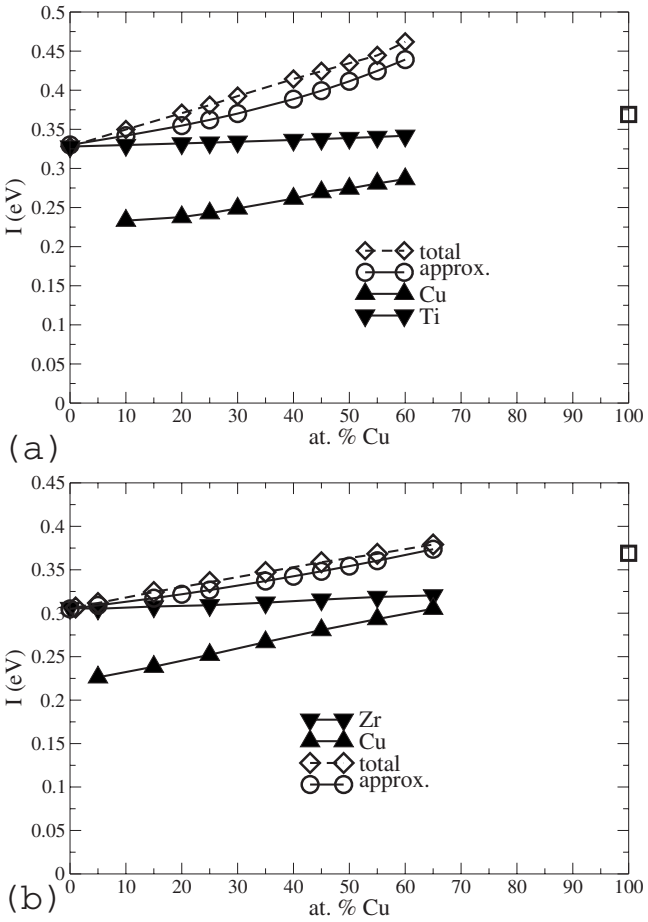

FIG. 8. Element-resolved and total calculated exchange integral I for fcc (a) Ti-Cu and (b) Zr-Cu alloys as a function of the Cu content. The I value for pure fcc-Cu (□) is taken from Ref. 51. The values introduced as circles (○) represent approximations for I by using Eq. (16).

B. Exchange integral I and Stoner enhancement S

According to Eq. (10), the determination of the spin susceptibility also requires the knowledge of the exchange integral I. Our calculated values of I for fcc-Ti and fcc-Zr are 0.330 and 0.305 eV, respectively. Former calculations yielded I=0.302 eV,[37] 0.339 eV,[51] and 0.290 eV (Ref. 53) for fcc-Ti and I=0.270 eV,[37] 0.305 eV,[51] and 0.245 eV (Ref. 53) for fcc-Zr. This parameter is not expected to depend sensitively on the atomic volume and was found not to vary significantly with crystal structure for these elements.[37] Our results are also well in line with previously calculated data. The exchange integral is smaller for fcc-Ti than for fcc-Zr, and this difference is again due to the higher atomic number of the latter metal.

The calculated effective I values for the four alloy systems are presented in Figs. 8 and 9. According to the discussion in the Appendix, it can be found from the values of the total enhanced and unenhanced spin susceptibilities of alloys. The element-projected exchange-correlation integrals I_α

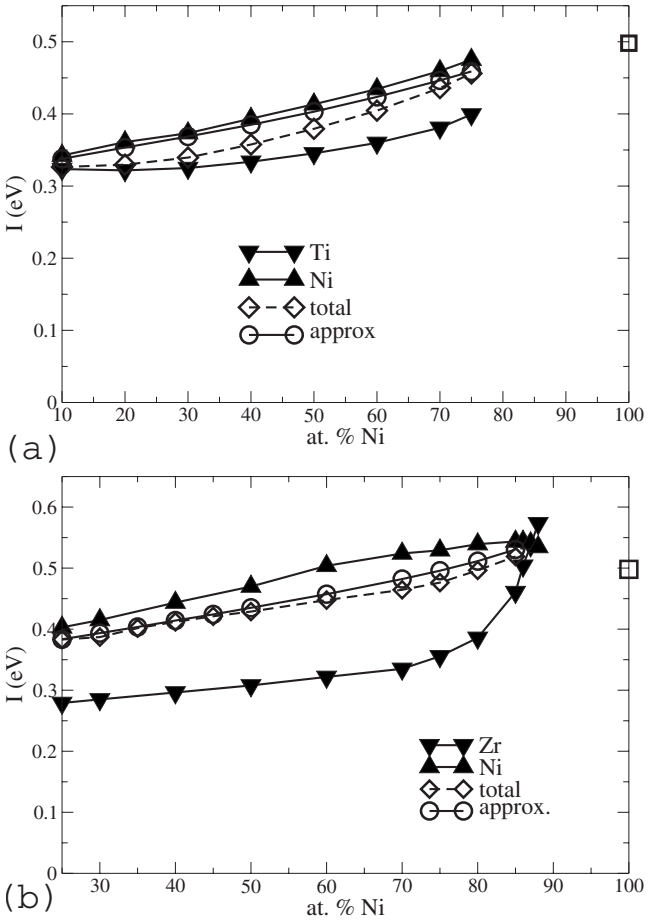

FIG. 9. Element-resolved and total calculated exchange integral I for fcc (a) Ti-Ni and (b) Zr-Ni alloys as a function of the Ni content. The I value for pure fcc-Ni (□) is taken from Ref. 51. The values introduced as circles (○) represent approximations for I by using Eq. (16).

are calculated under conditions when the intercomponent contributions to the element-projected susceptibility (connected with $\chi_{\alpha\beta}$) are neglected. As seen in Figs. 8 and 9, the element-projected exchange-correlation integrals I_α (α=Ti, Zr, Cu, or Ni) vary monotonically with alloy content.

In lack of a direct calculation of I for alloys, some assumption has usually been made previously in order to get an appropriate alloy average value by using the I values of the constituent metals. Bose *et al.*[36] suggested the following formula for estimating the exchange integral $I_{A\text{-}B}$ for an alloy A-B:

$$I_{A-B} = c_A \left[\frac{n_A(E_F)}{n(E_F)} \right]^2 I_A + c_B \left[\frac{n_B(E_F)}{n(E_F)} \right]^2 I_B, \qquad (16)$$

where c_A and c_B denote fractional compositions, I_A and I_B are the exchange integrals of the constituent pure metals, and $n_{A,B}(E_F)$ and $n(E_F)$ represent the element-resolved and total density of states at the Fermi level. By using the calculated partial density of states at the Fermi level (Figs. 6 and 7), we determined these approximate $I_{A\text{-}B}$ values for all four alloy systems and represented them in Figs. 8 and 9 by the symbols ○. We can see that in most cases, Eq. (16) indeed provides a good approximation for the average I value in an alloy.

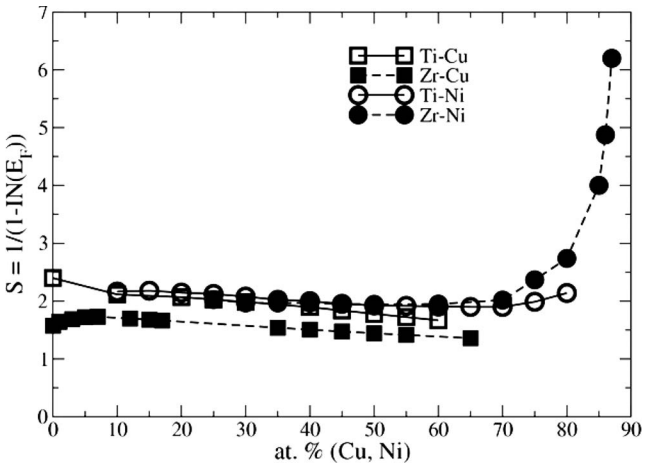

FIG. 10. Effective Stoner enhancement parameter S calculated for fcc Ti-Cu, Zr-Cu, Ti-Ni, and Zr-Ni alloys on the basis of Eq. (10) by using the calculated $n(E_F)$ and I values.

The enhancement of the spin susceptibility due to exchange-correlation effects is characterized by the Stoner enhancement factor S (Fig. 10), which is composed of $n(E_F)$ and I [see Eq. (10)]. By considering the composition dependence of the density of states and the exchange integral, we can see that, due to the slight variation of I only, the change of the effective S is mainly determined by the compositional variation of $n(E_F)$. Since the latter quantity decreases with increasing TL content (Cu or Ni) up to about 60–70 at. % TL, this is reflected in the composition dependence of S as well. However, for higher Ni contents in Ti-Ni and Zr-Ni alloys, there is a steep rise of S as the system approaches the critical concentration for the onset of ferromagnetism around 90 at. % Ni.

VI. COMPARISON OF CALCULATED AND EXPERIMENTAL SUSCEPTIBILITIES

The calculated element-resolved and total spin susceptibilities are shown in Figs. 11 and 12 for the four alloy systems. In line with the decrease of $n(E_F)$ and the weak composition dependence of I, the calculated χ_{spin} susceptibility shows a decrease with increasing Cu or Ni content up to about 60–70 at. % TL. Among the element-specific susceptibilities, the spin susceptibility of Ni in the Zr-Ni alloys shows the strongest composition dependence. This effect is connected with the correlations between the induced spin densities of different alloy components i and j as has already been discussed above.

In Figs. 11 and 12, the total calculated susceptibilities (χ_{total}) are also displayed together with the experimental susceptibility values from Fig. 1 (thick solid lines). The qualitative variation of χ_{total} and χ_{expt} agrees very well. However, the calculated values are somewhat smaller than the experimental ones for the Cu-based alloys, whereas the situation is just the opposite for the Ni-based alloys. With reference to Figs. 6 and 7, the difference between the calculated total and

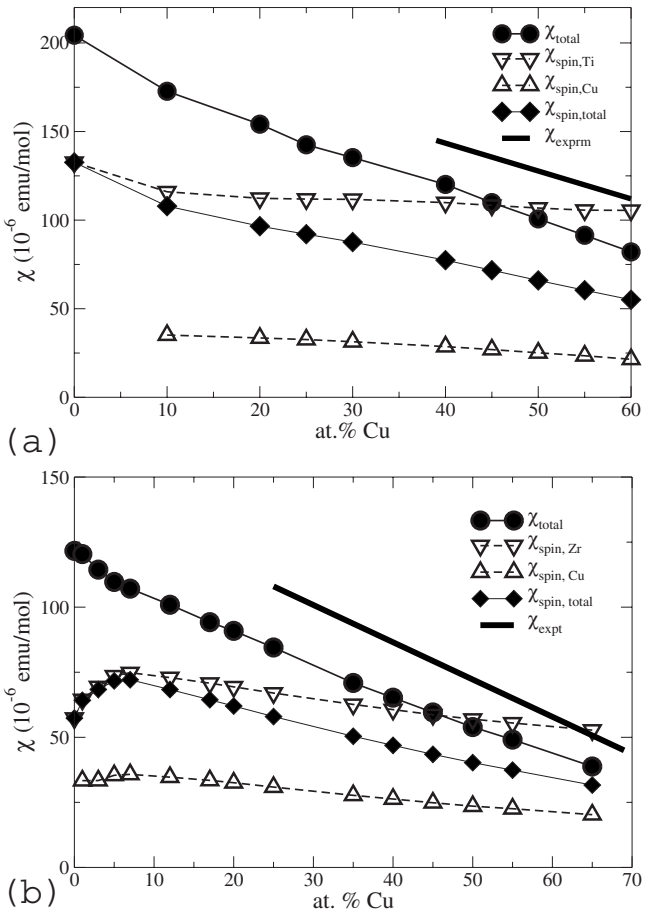

FIG. 11. Calculated element-resolved and total spin susceptibility χ_{spin} as well as total susceptibility χ_{total} for (a) fcc Ti-Cu alloys and (b) fcc Zr-Cu alloys as a function of the Cu content. The thick solid lines represent the average experimental susceptibility for the corresponding amorphous alloys from Fig. 1.

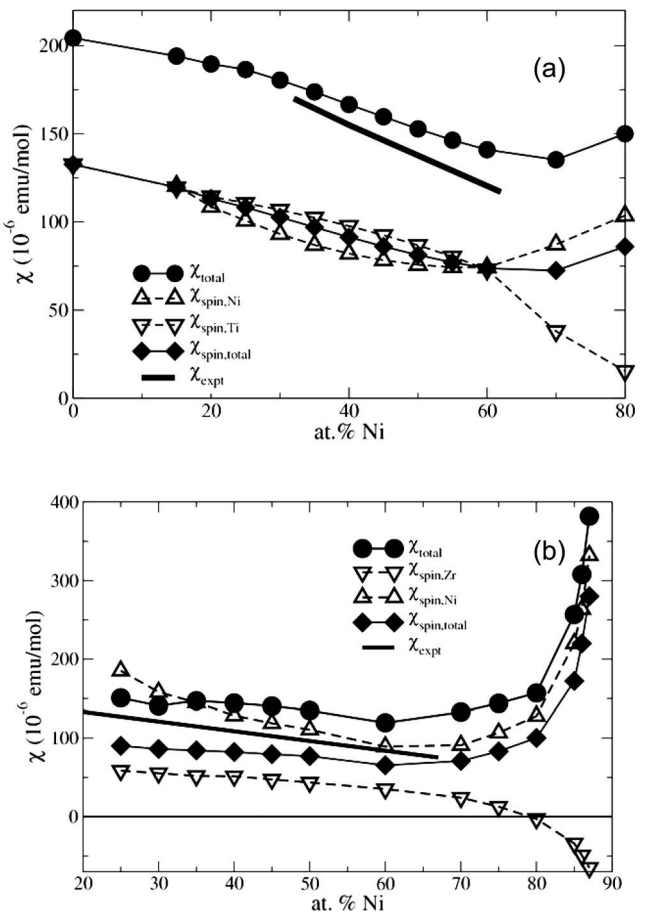

FIG. 12. Calculated element-resolved and total spin susceptibility χ_{spin} as well as total susceptibility χ_{total} for (a) fcc Ti-Ni alloys and (b) fcc Zr-Ni alloys as a function of the Ni content. The thick solid lines represent the average experimental susceptibility for the corresponding amorphous alloys from Fig. 1.

the experimental susceptibilities for a given alloy system reflects the deviation between the calculated and experimental $n(E_F)$ values.

Finally, we will make some notes on the Zr-Ni system partly because it behaves somewhat differently from the other alloy systems and partly also because in this system we have both calculated and experimental results for 90 at. % Ni where ferromagnetism appears.

One common feature of all TE-TL systems studied here is that the TE contribution to the total $n(E_F)$ is larger than the TL contribution up to about 70 at. % TL content except for the Zr-Ni system for which the reverse was obtained from our calculations for the fully disordered state. In former band-structure calculations of these TE-TL alloys when properly accounting for the CSRO, the Zr-Ni system did not behave differently in this respect. With reference to our attempts to account for some partial ordering in the Zr-Ni system [see Figs. 7(b) and 7(c)], this might give an explanation for our different result for Zr-Ni. In addition to $n(E_F)$, we compare in Fig. 13 also the enhanced spin susceptibility obtained in our calculations, with the data derived from the experiment and from the calculations with CSRO taken into account.[58] Experimental spin susceptibility was evaluated in two ways: (i) by correcting the experimental total susceptibility for the calculated orbital susceptibilities and (ii) deriving from the experimental $n(E_F)$ using the Stoner enhancement obtained in our calculations. In a similar way, we also evaluated another enhanced spin susceptibility which is based on the results of calculations accounting for CSRO.[58] These latter results are in agreement with experiment as was also the case for $n(E_F)$ in Fig. 7(b). If we accept that the χ_{spin} values derived from the experimental and theoretical literature $n(E_F)$ data are the correct ones, the χ_{spin} values derived by the use of our calculated total orbital susceptibility (thick solid lines in Fig. 13) are too small which may indicate that the latter quantity is apparently somewhat overestimated. On the other hand, the χ_{spin} values obtained directly in the present calculations appear as overestimated, evidently due to the too large $n(E_F)$ values for the chemically fully disordered state [using a CuAu-type structure with partial ordering improved our calculated $n(E_F)$ values as was shown in Fig. 7(b) and so would be also with our directly calculated χ_{spin} values].

Another point to note is that, due to hybridization effects, the spin susceptibility of Zr decreases with the increase of Ni concentration and changes sign around 80 at. % Ni. A further

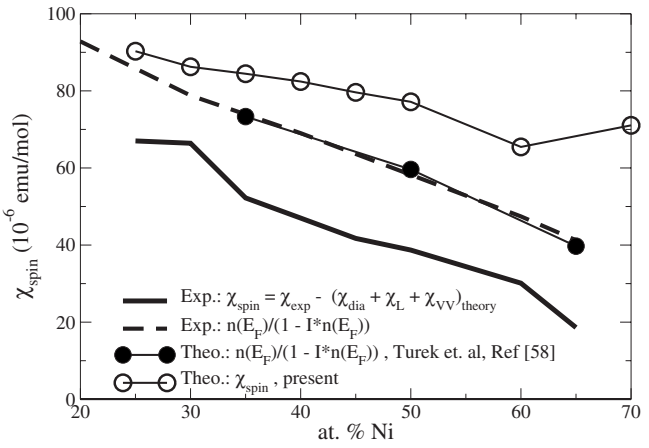

FIG. 13. Comparison of the enhanced spin susceptibilities of Zr-Ni alloys obtained by different methods: spin susceptibility obtained by correcting the experimental total susceptibility (χ_{spin}) for the calculated orbital ones (thick solid line), spin susceptibility derived from the experimental DOS(E_F) using the Stoner enhancement obtained in present calculations (dashed solid line), spin susceptibility derived in the same way but using the DOS(E_F) calculated accounting for CSRO (Ref. 58) (filled circles), and spin susceptibility obtained in the present calculations for the chemically fully disordered state (open circles).

decrease of the Zr content leads to an antiparallel alignment of Zr and Ni magnetic moments induced by the external magnetic field. At Ni concentrations higher than 80 at. % Ni, the Stoner enhancement increases to the extent that at about 90 at. % Ni, the condition of the Stoner instability of the paramagnetic state, $In(E_F) > 1$, is satisfied. The negative value of the spin susceptibility of Zr in Zr-Ni alloys at high Ni concentrations appears due to an intercomponent contribution discussed in the Appendix and is related to a high value of the Ni susceptibility as well as an antiferromagnetic intersite coupling of induced spin magnetic moments on the Zr and Ni sites.

The results of spin-polarized calculations for $Zr_{10}Ni_{90}$, in line with the calculations of the magnetic susceptibility for the paramagnetic state, also indicate the onset of ferromagnetism. We obtained a magnetic moment of 0.18 μ_B for Ni and −0.07 μ_B for Zr, corresponding to an average magnetic moment of μ_{the}=0.155 μ_B/atom for this alloy composition. Calculations were performed also for higher Ni contents, and correspondingly, larger average magnetic moments were obtained (e.g., μ_{the}=0.32 μ_B/atom for a-Zr_7Ni_{93}). It was found that for the fcc structure used, the degree of chemical ordering had very little influence only on the total magnetic moment. Although these calculated magnetic moments are apparently much higher than the experimental data for the same alloy compositions (e.g., μ_{expt}=0.041 μ_B/atom for the a-$Zr_{10}Ni_{90}$ alloy[4]), their composition dependence seems to yield a critical concentration for the onset of ferromagnetism slightly below 90 at. % Ni, in good agreement with experiments.[4]

VII. CONCLUSIONS

We have presented a detailed theoretical study of the magnetic susceptibility of the amorphous alloy systems a-Ti-Cu, a-Zr-Cu, a-Ti-Ni, and a-Zr-Ni. In order to keep the numerical effort at an acceptable level, an fcc structure with complete chemical disorder was used. These simplifications allowed us to calculate all contributions to the susceptibility, including the Landau contribution. It was found that the orbital susceptibilities give a significant contribution to the total one for the alloys studied. Our detailed results allowed us to check a number of simplifying assumptions previously made when dealing with the magnetic susceptibility of amorphous alloys. In particular, the use of an effective Stoner exchange integral I as suggested by Bose *et al.*[36] turned out to be fairly well justified. Our total magnetic susceptibility was found to deviate somewhat from the corresponding experimental values. This discrepancy can be primarily attributed to the fact that due to the structure used and due to the neglect of any chemical short-range order, in particular, in the case of the Ni-based alloys, our calculations could not properly account for the values of the electronic density of states at the Fermi level and, hence, provide the proper spin susceptibility values.

In an attempt for remedying some of these deficiencies, we have also made calculations for the Zr-Ni system by taking into account some partial ordering. The results obtained in this manner for $n(E_F)$ indicated better agreement with experimental data and with previous calculations performed by considering CSRO.

On the other hand, the trends in the variation of the susceptibility with composition are described for all systems rather well in our calculations. For that reason, it is assumed that this applies for the variations of orbital and spin contributions as well. In the Zr-Ni systems, calculations indicated the increase of the Stoner enhancement as the Ni content approaches 90 at. % Ni. In agreement with the experimental findings,[4] for the $Zr_{10}Ni_{90}$ alloy, our theoretical results have indeed shown the onset of a ferromagnetic state at this composition: The fulfillment of the Stoner criterion, i.e., $In(E_F) > 1$, indicated an instability of the paramagnetic state, whereas the spin-polarized calculations yielded a nonzero spontaneous magnetic moment.

ACKNOWLEDGMENT

This work was financed by the Deutsche Forschungsgemeinschaft (Project No. Eb154/9).

APPENDIX

Let us consider here in more detail the different mechanisms influencing the magnetic susceptibility. We deal first with the induced spin magnetic moment (for the sake of simplicity, we consider here only the spin magnetic moment) m^{α}_{spin} on the site α which can be represented according to Eq. (6) as follows:

$$m^{\alpha}_{spin} = -\frac{1}{\pi}\mathrm{Tr\ Im}\int^{E_F} dE \int_{\Omega_\alpha} d^3r \sum_{\beta} \int_{\Omega_\alpha} d^3r' \beta\mu_B\sigma_z \times G(\mathbf{r},\mathbf{r}',E)\Delta\mathcal{H}_{spin}G(\mathbf{r}',\mathbf{r},E)$$

$$= -\frac{1}{\pi}\mathrm{Tr\ Im}\int^{E_F} dE \int_{\Omega_\alpha} d^3r \beta\mu_B\sigma_z G(\mathbf{r},\mathbf{r},E)$$

$$\times[\beta\sigma_z\mu_B B_{\text{ext}} + \Delta\mathcal{H}^{\text{xc}\alpha}_{\text{spin}}(\mathbf{r}')]G(\mathbf{r},\mathbf{r},E)$$
$$-\frac{1}{\pi}\text{Tr Im}\int^{E_F} dE\int_{\Omega_0} d^3r\sum_{\beta\neq\alpha}\int_{\Omega_\beta}$$
$$\times d^3r'\,\beta\mu_B\sigma_z G(\mathbf{r},\mathbf{r}',E)[\beta\sigma_z\mu_B B_{\text{ext}}$$
$$+\Delta\mathcal{H}^{\text{xc}\beta}_{\text{spin}}(\mathbf{r}')]G(\mathbf{r}',\mathbf{r},E). \quad \text{(A1)}$$

This expression leads to a corresponding spin susceptibility

$$\chi^{\alpha}_{\text{spin}} = -\frac{\mu_B^2}{\pi}\text{Tr Im}\int^{E_F} dE\int_{\Omega_\alpha} d^3r\beta\sigma_z G(\mathbf{r},\mathbf{r},E)[\beta\sigma_z$$
$$+\beta\sigma_z K^{\text{xc}\alpha}_{\text{spin}}(\mathbf{r})\gamma^{\alpha}(\mathbf{r})\chi^{\alpha}_{\text{spin}}]G(\mathbf{r},\mathbf{r},E)$$
$$-\frac{\mu_B^2}{\pi}\text{Tr Im}\int^{E_F} dE\int_{\Omega_\alpha} d^3r\sum_{\beta\neq\alpha}\int_{\Omega_\beta} d^3r'\beta\sigma_z G(\mathbf{r},\mathbf{r}',E)$$
$$\times[\beta\sigma_z + \beta\sigma_z K^{\text{xc}\beta}_{\text{spin}}(\mathbf{r})\gamma^{\beta}(\mathbf{r})\chi^{\beta}_{\text{spin}}]G(\mathbf{r}',\mathbf{r},E). \quad \text{(A2)}$$

This equation can be written in terms of the magnetic susceptibility in the following way:

$$\chi^{\alpha}_{\text{spin}} = \chi^{0,\alpha}_{\text{spin}} + \chi^{0,\alpha}_{\text{spin}} I_\alpha \chi^{\alpha}_{\text{spin}} + \sum_{\beta\neq\alpha}[\chi^{0,\alpha\beta}_{\text{spin}} + \chi^{0,\alpha\beta}_{\text{spin}} I_\beta \chi^{\beta}_{\text{spin}}], \quad \text{(A3)}$$

where

$$\chi^{0,\alpha\beta}_{\text{spin}} = -\frac{\mu_B^2}{\pi}\text{Tr Im}\int^{E_F} dE\int_{\Omega_\alpha} d^3r\int_{\Omega_\beta}$$
$$\times d^3r'\,\beta\sigma_z G(\mathbf{r},\mathbf{r}',E)\beta\sigma_z G(\mathbf{r}',\mathbf{r},E),$$

$$\chi^{0,\alpha\alpha}_{\text{spin}} \equiv \chi^{0,\alpha}_{\text{spin}}. \quad \text{(A4)}$$

The term $\chi^{0,\alpha\beta}_{\text{spin}}$ describes the change of spin magnetic moment on site α appearing due to interaction of external magnetic field with the electrons on site β.

When dealing with a disordered alloy system, the average spin susceptibility on site α can be represented through the element-projected values

$$\chi^{\alpha}_{\text{spin}} = \sum_n x_n \chi^{n,\alpha}_{\text{spin}},$$

where x_n is the concentration of component n. Then, one can write the element-projected susceptibility on site α?(omitting the index α)

$$\chi^{n}_{\text{spin}} = \chi^{0,n}_{\text{spin}} + \chi^{0,n}_{\text{spin}} I_n \chi^{n}_{\text{spin}} + \sum_{m\neq n} x_m \chi^{0,nm}_{\text{spin}}[1 + I_m\chi^{m}_{\text{spin}}]. \quad \text{(A5)}$$

The problem for calculation of configurational average where the site α is occupied by the atoms A_n with corresponding concentration, has been considered by Staunton.[24]

The system of equations (A5) [as well as system of Eq. (A3) for the ordered compounds] for the different alloy components should be solved self-consistently, as was mentioned already in Sec. III A. However, for our present analysis, let us represent Eq. (A5) in the following form:

$$\chi^{n}_{\text{spin}} = \frac{\chi^{0,n}_{\text{spin}}}{1 - I_n\chi^{0,n}_{\text{spin}}} + \sum_{m\neq n} x_m \chi^{0,nm}_{\text{spin}} \frac{1 + I_m\chi^{m}_{\text{spin}}}{1 - I_n\chi^{0,n}_{\text{spin}}}. \quad \text{(A6)}$$

When the system under consideration is far from the Stoner instability, then, taking into account the small magnitude of $\chi^{0,nm}_{\text{spin}}$ and, therefore, keeping only the terms linear with respect to $\chi^{0,nm}_{\text{spin}}$, one can write Eq. (A6) as follows:

$$\chi^{n}_{\text{spin}} = \tilde{\chi}^{n}_{\text{spin}} + \sum_{m\neq n} x_m \chi^{0,nm}_{\text{spin}} \frac{1 + I_m\tilde{\chi}^{m}_{\text{spin}}}{1 - I_n\chi^{0,n}_{\text{spin}}}, \quad \text{(A7)}$$

where

$$\tilde{\chi}^{n}_{\text{spin}} = \frac{\tilde{\chi}^{0,n}_{\text{spin}}}{1 - I_n\chi^{0,n}_{\text{spin}}}. \quad \text{(A8)}$$

Thus, the second term in Eq. (A7) describes a contribution to the spin susceptibility of alloy component n which appears due to hybridization of the electronic states of different alloy components.

In the case, when at least one component is close to the Stoner instability, the second term in Eq. (A6) will have a significant value and, as a consequence, it will give an essential contribution to the component-projected magnetic susceptibilities. Depending on the sign of $\chi^{0,nm}_{\text{spin}}$, it can either increase or decrease these values. This effect can also change the sign of the magnetic moment of one of the alloy components, which means an antiparallel alignment of induced spin magnetic moments on the different alloy components.

The total spin susceptibility of an alloy (χ_{spin}) can be represented through the total unenhanced susceptibility (χ^{0}_{spin}) and effective Stoner exchange-correlation integral I,

$$\chi_{\text{spin}} = \frac{\chi^{0}_{\text{spin}}}{1 - I\chi^{0}_{\text{spin}}}. \quad \text{(A9)}$$

By taking into account Eq. (A6) one can see that this effective Stoner integral I depends in a complex way on the values of the Stoner integrals of the different alloy components. However, it can be evaluated in a simple way when the values of χ_{spin} and χ^{0}_{spin} are known. Note that the magnitude of the effective Stoner integral I is expected to be in good agreement with that obtained from Eq. (16) since they are determined within similar approximations.

*sergiy.mankovskyy@cup.uni-muenchen.de

[1] I. Bakonyi, J. Non-Cryst. Solids **180**, 131 (1995).

[2] For detailed references on band-structure calculations and photoemission experiments on amorphous TE-TL alloys, see Ref. 1.

[3] I. Bakonyi, V. Skumryev, R. Reisser, G. Hilscher, L. K. Varga, L. F. Kiss, H. Kronmüller, and R. Kirchheim, Z. Metallkd. **88**, 117 (1997).

[4] I. Bakonyi, L. F. Kiss, E. Varga, and L. K. Varga, Phys. Rev. B **71**, 014402 (2005).

[5] S. Kanemaki, M. Suzuki, Y. Yamada, and U. Mizutani, J. Phys. F: Met. Phys. **18**, 105 (1988).

[6] U. Mizutani, N. Akutsu, and T. Mizoguchi, J. Phys. F: Met. Phys. **13**, 2127 (1983).

[7] E. Babic, R. Ristic, M. Miljak, M. G. Scott, and G. Gregan, Solid State Commun. **39**, 139 (1981).

[8] Z. Altounian and J. O. Strom-Olsen, Phys. Rev. B **27**, 4149 (1983).

[9] I. Bakonyi, H. Ebert, J. Voitländer, K. Tompa, A. Lovas, G. Konczos, P. Bánki, and H. E. Schone, J. Appl. Phys. **61**, 3664 (1987).

[10] R. Ristic, Z. Marohnic, and E. Babic, Fiz. A **12**, 89 (2003).

[11] I. Kokanovic, B. Leontic, and J. Lukatela, Phys. Rev. B **41**, 958 (1990).

[12] I. R. Szofran, G. R. Gruzalski, J. W. Weymouth, and D. J. Sellmyer, Phys. Rev. B **14**, 2160 (1976).

[13] E. Babic, R. Ristic, M. Miljak, and M. G. Scott, in *Proceedings of the Fourth International Conference on Rapidly Quenched Metals, Sendai, 1981* edited by T. Masumoto and K. Suzuki (The Japan Institute of Metals, Sendai, 1982), p. 1079.

[14] R. Ristic, E. Babic, K. Saub, and M. Miljak, Fizika (Zagreb) **15**, 363 (1983).

[15] H. J. Eifert, B. Elschner, and K. H. J. Buschow, Phys. Rev. B **25**, 7441 (1982).

[16] K. H. J. Buschow and N. M. Beekmans, Phys. Rev. B **19**, 3843 (1979).

[17] H. J. Eifert, B. Elschner, and K. H. J. Buschow, Phys. Rev. B **29**, 2905 (1984).

[18] I. Nagy, I. Bakonyi, A. Lovas, E. Tóth-Kádár, K. Tompa, M. Hossó, Á. Cziráki, and B. Fogarassy, J. Less-Common Met. **167**, 283 (1991).

[19] T. Mizoguchi and T. Kudo, in AIP Conf. Proc. No. 29 (AIP, New York, 1976), p. 167; quoted also by T. Mizoguchi, S. von Molnar, G. S. Cargill III, T. Kudo, N. Shiotani, and H. Sekizawa, in *Amorphous Magnetism II*, edited by R. A. Levy and R. Hasegawa (Plenum, New York, 1977), p. 513.

[20] A. Amamou and G. Krill, Solid State Commun. **28**, 957 (1978).

[21] A. Amamou, R. Kuentzler, Y. Dossmann, P. Forey, J. L. Glimois, and J. L. Feron, J. Phys. F: Met. Phys. **12**, 2509 (1982).

[22] Z. F. Dong, K. Lu, R. Lück, I. Bakonyi, and Z. Q. Hu, Nanostruct. Mater. **9**, 363 (1997).

[23] H. C. Jamieson and F. D. Manchester, J. Phys. F: Met. Phys. **2**, 323 (1972).

[24] J. Staunton, Ph.D. thesis, University of Bristol, 1982; M. Matsumoto, J. B. Staunton, and P. Strange, J. Phys.: Condens. Matter **2**, 8365 (1990).

[25] M. Deng, H. Freyer, and H. Ebert, Solid State Commun. **114**, 365 (2000); M. Deng, H. Freyer, J. Voitländer, and H. Ebert, J. Phys.: Condens. Matter **13**, 8551 (2001); H. Ebert, S. Mankovsky, H. Freyer, and M. Deng, *ibid.* **15**, S617 (2003); S. Mankovsky and H. Ebert, Phys. Rev. B **69**, 014414 (2004); **74**, 054414 (2006).

[26] J. Benkowitsch and H. Winter, J. Phys. F: Met. Phys. **13**, 991 (1983).

[27] M. Yasui and M. Shimizu, J. Phys. F: Met. Phys. **15**, 2365 (1985).

[28] O. Gunnarsson, J. Phys. F: Met. Phys. **6**, 587 (1976).

[29] J. F. Janak, Phys. Rev. B **16**, 255 (1977).

[30] W. H. Butler, Phys. Rev. B **31**, 3260 (1985).

[31] M. S. S. Brooks, Physica B & C **130**, 6 (1985).

[32] L. D. Landau, Z. Phys. **64**, 629 (1930).

[33] I. Bakonyi, Acta Mater. **53**, 2509 (2005).

[34] S. Brauer, J. O. Strom-Olsen, M. Sutton, Y. S. Yang, A. Zaluska, G. B. Stephenson, and U. Köster, Phys. Rev. B **45**, 7704 (1992).

[35] V. L. Moruzzi, P. Oelhafen, A. R. Williams, R. Lapka, H.-J. Güntherodt, and J. Kübler, Phys. Rev. B **27**, 2049 (1983).

[36] S. K. Bose, J. Kudrnovsky, F. S. Razavi, and O. K. Andersen, Phys. Rev. B **43**, 110 (1991).

[37] I. Bakonyi, H. Ebert, and A. I. Liechtenstein, Phys. Rev. B **48**, 7841 (1993).

[38] S. K. Bose, L. E. Ballentine, and J. E. Hammerberg, J. Phys. F: Met. Phys. **13**, 2089 (1983).

[39] W. Jank, Ch. Hausleitner, and J. Hafner, J. Phys.: Condens. Matter **3**, 4477 (1991).

[40] P. R. Peduto, S. Frota-Pessóa, and M. S. Methfessel, Phys. Rev. B **44**, 13283 (1991).

[41] A. Pasquarello, K. Laasonen, R. Car, C. Lee, and D. Vanderbilt, Phys. Rev. Lett. **69**, 1982 (1992).

[42] D. Nguyen Manh, D. Mayou, F. Cyrot-Lackmann, and A. Pasturel, J. Phys. F: Met. Phys. **17**, 1309 (1987).

[43] A. Lee, G. Etherington, and C. N. J. Wagner, J. Non-Cryst. Solids **61-62**, 349 (1984); S. Lefebvre, A. Quivy, J. Bigot, Y. Calvayrac, and R. Bellissent, J. Phys. F: Met. Phys. **15**, L99 (1985).

[44] Ch. Hausleitner and J. Hafner, Phys. Rev. B **42**, 5863 (1990); Ch. Hausleitner and J. Hafner, *ibid.* **45**, 115 (1992).

[45] J. Banhart, H. Ebert, J. Voitländer, and H. Winter, J. Magn. Magn. Mater. **61**, 221 (1986).

[46] P. W. Selwood, *Magnetochemistry* (Interscience, New York, 1956); E. König and G. König, in *Magnetic Properties of Coordination and Organometallic Transition Metal Compounds*, edited by K. H. Hellwege and A. M. Hellwege, Landolt-Börnstein, New Series, Group II, (Springer, Berlin, 1979), Vol. II/10, p. 12.

[47] E. Batalla, Z. Altounian, and J. O. Strom-Olsen, Phys. Rev. B **31**, 577 (1985).

[48] R. Ristic, Z. Marohnic, and E. Babic, in *Properties and Applications of Nanocrystalline Alloys from Amorphous Precursors*, edited by B. Idzikowski, P. Švec, and M. Miglierini, NATO Science Series II (Kluwer, Dordrecht, 2005), Vol. 184, p. 363.

[49] R. Ristic and E. Babic, Fiz. A **14**, 97 (2005).

[50] C. M. Place and P. Rhodes, Phys. Status Solidi B **47**, 475 (1971).

[51] V. L. Moruzzi, J. F. Janak, and A. R. Williams, *Calculated Electronic Properties of Metals* (Pergamon, New York, 1978).

[52] D. A. Papaconstantopoulos, L. L. Boyer, B. M. Klein, A. R. Williams, V. L. Moruzzi, and J. F. Janak, Phys. Rev. B **15**, 4221 (1977).

[53] M. M. Sigalas, D. A. Papaconstantopoulos, and N. C. Bacalis, Phys. Rev. B **45**, 5777 (1992); M. M. Sigalas and D. A. Papaconstantopoulos, Phys. Rev. B **50**, 7255 (1994).

[54] This value corresponding to the condition $V_{\mathrm{fcc}}=V_{\mathrm{hcp}}$ was obtained by scaling up the result calculated in Ref. 37 (1.55 states/eV atom for a lattice parameter $a_{\mathrm{fcc}}=0.4006$) on the

basis of the relation $n(E_F) \propto V^{5/3}$, which is usually considered to be valid for the *d*-band metals; see V. Heine, in *The Physics of Metals*, edited by J. M. Ziman (Cambridge University Press, London, 1968), Vol. 1, p. 1;; O. K. Andersen, W. Klose, and H. Nohl, Phys. Rev. B **17**, 1209 (1978).

[55] D. Nguyen Manh, D. Mayou, D. Pavuna, and F. Cyrot-Lackmann, Phys. Scr., T **13**, 230 (1986); F. Cyrot-Lackmann, D. Mayou, and D. Nguyen Manh, Mater. Sci. Eng., A **99**, 245 (1988).

[56] D. Nguyen Manh, D. Pavuna, F. Cyrot-Lackmann, D. Mayou, and A. Pasturel, Phys. Rev. B **33**, 5920 (1986).

[57] A. Pasturel and J. Hafner, Phys. Rev. B **34**, 8357 (1986).

[58] I. Turek, Ch. Becker, and J. Hafner, J. Phys.: Condens. Matter **4**, 7257 (1992).

[59] J. Duarte Jr. and S. Frota-Pessoa, Z. Phys. Chem., Neue Folge **157**, 503 (1988).